# Membrane- and plate-type acoustic metamaterials

Tai-Yun Huang, Chen Shen, and Yun Jing[a)]
*Department of Mechanical and Aerospace Engineering, North Carolina State University, Raleigh, North Carolina 27695, USA*

(Received 29 September 2015; revised 28 January 2016; accepted 15 March 2016; published online 30 June 2016)

Over the past decade there has been a great amount of research effort devoted to the topic of acoustic metamaterials (AMMs). The recent development of AMMs has enlightened the way of manipulating sound waves. Several potential applications such as low-frequency noise reduction, cloaking, angular filtering, subwavelength imaging, and energy tunneling have been proposed and implemented by the so-called membrane- or plate-type AMMs. This paper aims to offer a thorough overview on the recent development of membrane- or plate-type AMMs. The underlying mechanism of these types of AMMs for tuning the effective density will be examined first. Four different groups of membrane- or plate-type AMMs (membranes with masses attached, plates with masses attached, membranes or plates without masses attached, and active AMMs) will be reviewed. The opportunities, limitations, and challenges of membrane- or plate-type AMMs will be also discussed. © *2016 Acoustical Society of America*. [http://dx.doi.org/10.1121/1.4950751]

[MRH] Pages: 3240–3250

## I. INTRODUCTION

In recent years, metamaterials have drawn a lot of attention in the scientific community due to their unusual properties and useful applications. Metamaterials are artificial materials made of subwavelength microstructures. They are well known to exhibit exotic properties and could manipulate wave propagation in a way that is impossible by using nature materials. Metamaterials were first considered from the idea of simultaneously negative dielectric constant ($\varepsilon$) and magnetic permeability ($\mu$) for electromagnetic (EM) waves.[1] Later on, Pendry *et al*. presented the first man-made structure to achieve negative permeability and also showed that the negative refractive could be fulfilled by a periodic structure.[2] These two seminal papers opened up a new field and have driven a vast number of researches on EM metamaterials such as breaking the diffraction limitation for imaging,[3] cloaking EM waves,[4] and ultra-broadband light absorption.[5] The ideas of creating acoustic metamaterials (AMMs)[6–8] and elastic wave metamaterials[9–11] follows those of EM metamaterials thanks to concept analogy. AMMs can achieve not only negative acoustic properties that do not exist in nature but also cloaking,[12] subwavelength imaging,[13] anomalous refraction/reflection,[14] one-way transmission,[15] and focusing,[16] etc. The effective mass density of AMMs plays an important role to achieve these unusual phenomena. Therefore, a number of AMMs have been proposed to tune the effective density to extreme values, including negative[17] and near-zero values,[18] or to achieve highly anisotropic density.[19] The very first approach utilized composite materials composed of lead balls, epoxy, and rubber.[6,20] Negative density can be induced by the local-resonance of this structure. Since then, other novel AMMs have emerged in this area, such as perforated plate type AMMs (Refs. 12 and 21) and space-coiling type AMMs.[14,16,22–25] In this paper, a specific type of AMMs, i.e., the membrane- and plate-type AMMs, will be reviewed. Compared with other AMMs, this type of AMM is in general light-weight, which is particularly important for noise control. They also have relatively simple geometries and the ability to actively tune the effective density. Most importantly and uniquely, a broadband negative effective density can be observed with very low loss[26] if properly designed. Thus, they have generated a large interest in the AMM community to explore their theory, mechanism, and applications. A variety of designs based on the membrane- and plate-type AMMs have been proposed and implemented to explore and expand their applications. Four different groups of membrane- and plate-type AMMs will be discussed and they are as follows: membranes with masses attached, plates with masses attached, membranes or plates without masses attached, and active AMMs. These AMMs have found applications in low-frequency sound attenuation,[27–29] cloaking,[30] angular filtering,[31] subwavelength imaging,[32] energy tunneling,[18] etc. Unlike membrane-type AMMs which mainly manipulate the transmission, reflection, and absorption of acoustic waves, plates with attached masses could control either the acoustic waves interacting with them or elastic waves propagating within the plates (e.g., flexural and lamb waves). For instance, attaching a two-dimensional (2D) array of composite stubs[33–37] on the surface of a thin plate could manipulate the plate's lamb modes. This paper, however, focuses on the plate-type AMMs for manipulating acoustic waves.

The paper is structured as follows: Section II introduces the theoretical background of membrane- and plate-type AMMs for tuning the effective density. Section III reviews different designs of membrane- and plate-type AMMs and their applications. Section IV discusses opportunities, limitations, and challenges of membrane- and plate-type AMMs.

[a)]Electronic mail: yjing2@ncsu.edu

 0001-4966/2016/139(6)/3240/11/$30.00 

## II. EFFECTIVE DENSITY OF MEMBRANE- AND PLATE-TYPE AMMS

To begin, it is useful and important to understand the mechanism of membrane- and plate-type AMMs for tuning the effective density. Two simple yet representative examples are illustrated in Figs. 1(a) and 1(b), where a membrane or a thin plate is clamped inside a subwavelength waveguide, with or without a mass attached, under the excitation of plane waves. When the membrane (plate) vibrates under the acoustic excitation, the effective/dynamic density arises due to the restoring force associated with this structure, as will be detailed below. These AMMs have been adopted in Refs. 27, 38, and 39 and many other papers that will be reviewed here.

We first discuss the case without masses attached on the membrane or plate [Fig. 1(a)]. For a vibrational thin plate under acoustic excitation, the governing equation can be written as

$$D\nabla^4 W(x,y,t) + \rho h \frac{\partial^2 W(x,y,t)}{\partial t^2} = P(x,y,t), \tag{1}$$

where $x$ and $y$ are the spatial coordinates on the plate; $t$ is time; $D$ is the flexural rigidity and $D = Eh^3/12(1-v^2)$; $P$ is the external pressure; $E$, $v$, $\rho$, and $h$ are the Young's modulus, Poisson's ratio, density, and thickness of the plate, respectively.

For a vibrational membrane under acoustic excitation, the governing equation reads

$$T\nabla^2 W_1(x,y,t) - \rho_1 h_1 \frac{\partial^2 W_1(x,y,t)}{\partial t^2} = -P_1(x,y,t), \tag{2}$$

where $T$ is the uniform tension per unit length; $P_1$ is the external pressure; $\rho_1$ and $h_1$ are the density and thickness of the membrane, respectively. As can be seen from Eqs. (1) and (2), in general, the vibrational response of a membrane is intrinsically dictated by the tension applied whereas the vibrational response of a thin plate is dominated by its stiffness. This distinguishes the membrane-type AMMs from the plate-type AMMs (although on many occasions, the word "membrane" has been used to describe a thin plate[19,32]). Equations (1) and (2) can be solved either numerically or analytically (e.g., for a circular thin plate) and the effective density can be estimated for the AMM. For example, the transverse displacement and acceleration could be obtained and the effective mass density could be calculated by

$$\rho_{\text{eff}} = (\bar{p}_1 - \bar{p}_2)/\bar{a}_z, \tag{3}$$

where $\bar{p}_1$ and $\bar{p}_2$ are the surface integrations of pressures over the left and right surfaces, respectively, of the membrane or plate and $\bar{a}_z$ is the volume integration of the normal acceleration of the membrane or plate. For the AMM shown in Fig. 1(a), the effective density has been shown to follow the Drude form and could be written as[27]

$$\rho_{\text{eff}} = \rho'\left(1 - \frac{{\omega_c}^2}{\omega^2}\right), \tag{4}$$

where $\rho'$ is the average density of the air loaded with the membrane or plate and $\omega_c$ is the first resonance frequency of the membrane or plate. We note that Eq. (4) has only been proved valid for air. For other fluids, such as water, the effect of the fluid loading on the membrane or plate is much stronger and Eq. (4) may possibly need to be revised. Clearly, at a frequency below the first resonance frequency, the effective density is negative, therefore resulting in a broadband negative density AMM. Within this frequency range, the acceleration of the membrane or plate is found to be out-of-phase with respect to the external excitation.[27] Close to the resonance frequency, the effective density is near-zero. A figure showing the effective density of a clamped, thin plate can be found in Fig. 2. Alternatively, the effective density of this AMM can be understood by a mass-spring system as shown in Fig. 1(c).[29] In the system, a mass $m$ is confined by two springs $G$ fixed to the ground. The effective mass of a one-dimensional (1D) lattice system composed of this unit cell reads

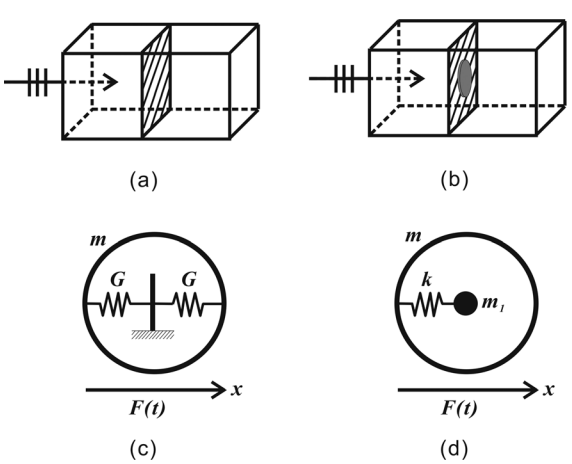


FIG. 1. A membrane or plate clamped in a waveguide. (a) Without mass attached. (b) With mass attached. (c) The corresponding mass-spring diagram for (a). (d) The corresponding mass-spring diagram for (b).

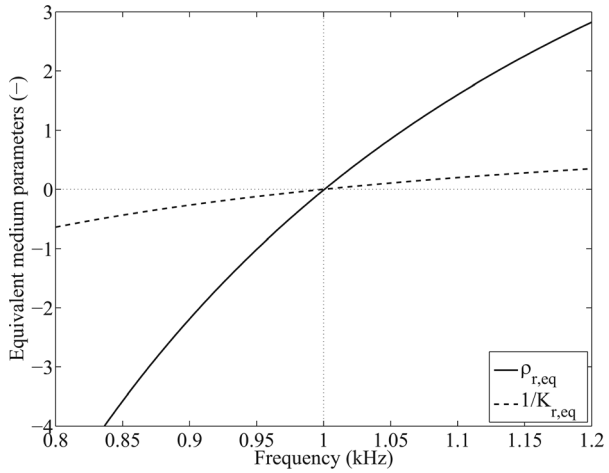


FIG. 2. The normalized effective density (solid line) and bulk modulus (dashed line) of a thin plate-type AMM with open channels. Taken from Bongard *et al.* (Ref. 38).

$$m_{\text{eff}} = m\left(1 - \frac{{\omega_0}^2}{\omega^2}\right), \tag{5}$$

where $\omega_0 = \sqrt{2G/m}$. Equation (5) is in the same form with Eq. (4). In the membrane- or plate-type AMM, the membrane or plate behaves as the springs and the masses. They are clamped on the boundaries just as the springs are fixed to the ground.

For the membrane- or plate-type AMMs with mass attached shown in Fig. 1(b), the vibrational governing equations become more complicated. For example, for a membrane with a mass attached, the governing equation reads[40]

$$\rho_1 h_1 \frac{\partial^2 W_1(x,y,t)}{\partial t^2} - T\nabla^2 W_1(x,y,t) = p_1 - p_2 + \sum_{i=1}^{I} Q_i(t)\delta(x - x_i)\delta(y - y_i), \tag{6}$$

where $p_1 - p_2$ is the net acoustic pressure applied on the membrane and the third term on the right-hand side of the equation is the summation of point forces ($Q_i$) at collocation points ($I$) on the interface between the membrane and mass; $\delta$ is the Dirac delta function.

For a plate with multiple masses attached, the governing equation can be written as[41]

$$D'\nabla^4 W(x,y,t) - T\nabla^2 W(x,y,t) + \rho h \frac{\partial^2 W(x,y,t)}{\partial t^2} = p_1 - p_2 + \sum_{s=1}^{S}\sum_{i=1}^{I} F_i^{(s)}\delta\left(x - x_i^{(s)}\right)\delta\left(y - y_i^{(s)}\right), \tag{7}$$

where $D' = D + (\sigma_0 h^3/12)$ is the effective bending stiffness, $\sigma_0$ is the initial stress on the plate; the inner summation ($i$) is similar to the summation in Eq. (6); the outer summation ($s$) accounts for multiple masses attached at different positions on the plate. Compared with Eq. (1) for plates, Eq. (7) includes the initial tension term (the second term on the left-hand side of the equation) and therefore is more generic.

Similarly, these governing equations can be solved and the effective density can be evaluated by using Eq. (3) or other approaches. In contrast to the membrane- or plate-type AMMs without mass attached, where deep/large negative density could occur within a broadband frequency, the addition of the mass introduces a resonance-based, relatively narrow frequency band negative density. For example, Yang *et al.*[39] observed that deep negative density occurs around the anti-resonance frequency, i.e., a frequency between the first and second resonance frequencies of the membrane with a mass attached. The corresponding effective density is shown in Fig. 3.[42] A mass-spring system has also been established to understand this resonance-based negative density. As can be seen in Fig. 1(d), an inner mass $m_1$ is connected to an outer mass $m$ through a spring $k$ and the effective mass can be written as[43]

$$m'_{\text{eff}} = m + \frac{m_1 {\omega_0}^2}{{\omega_0}^2 - \omega^2}, \tag{8}$$

where $\omega_0 = \sqrt{k/m_1}$. In the absence of loss, this effective mass is in the Lorentz form.

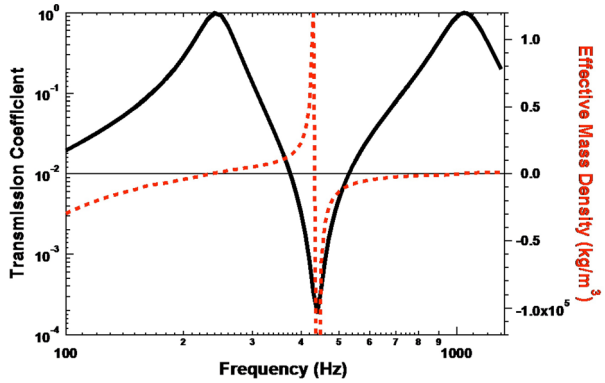


FIG. 3. (Color online) The transmission coefficient (solid line), which is the ratio of the magnitude of the transmitted pressure to the magnitude of the incident pressure, and effective mass density (dashed line) of a membrane-type AMM with mass attached are shown. The negative effective mass density occurs below the first resonance frequency (231 Hz) and the region between the anti-resonance frequency (448 Hz) and the second resonance frequency (1053 Hz). Taken from Ma (Ref. 42).

## III. DIFFERENT DESIGNS OF MEMBRANE- AND PLATE-TYPE AMMS AND THEIR POTENTIAL APPLICATIONS

### A. Membrane-type AMMs with masses attached

Yang *et al.*[39] demonstrated the first membrane-type AMMs [similar to that shown in Fig. 1(b)]. It was found that a stretched membrane with different masses attached could produce different vibrational modes with corresponding different transmission behaviors. In general, two peaks and one dip in between can be observed in the sound transmission curve below the second resonance frequency. While the peaks were caused by the two eigenmodes, the dip was due to the anti-resonance (both eigenmodes are excited but with opposite phase). At the two eigenmode frequencies, the average displacements on the membrane were relatively large, leading to high transmission. At the transmission dip frequency, the average displacement was minimum, which was responsible for the low sound transmission and large sound reflection. The extremely low sound transmission at this very low frequency was found to break the well-known mass law (Fig. 4). By tuning the mass attached on the membrane, the transmission curve can be tailored. For instance, by increasing the weight of the mass, the two peaks will shift to lower frequencies.

Later on, Yang *et al.*[44] extended their work to an array of membranes with attached masses which could be used for light-weight low-frequency sound reduction. Furthermore, to achieve broadband sound reduction, several AMM panels with different mass weights were stacked up. An average sound transmission loss (STL) >40 dB was achieved over the 50–1000 Hz frequency range with stacked panels thinner than 60 mm and lighter than 15 kg/m$^2$. The STL of this type of AMMs was further investigated numerically and experimentally by Naify *et al.*[45] by varying the mass and tension on the membrane. The corresponding out-of-plane displacement of the membrane was measured by a laser vibrometer. Naify *et al.*[46] later changed the geometry of the attached masses to coaxial rings. Samples with a different number of

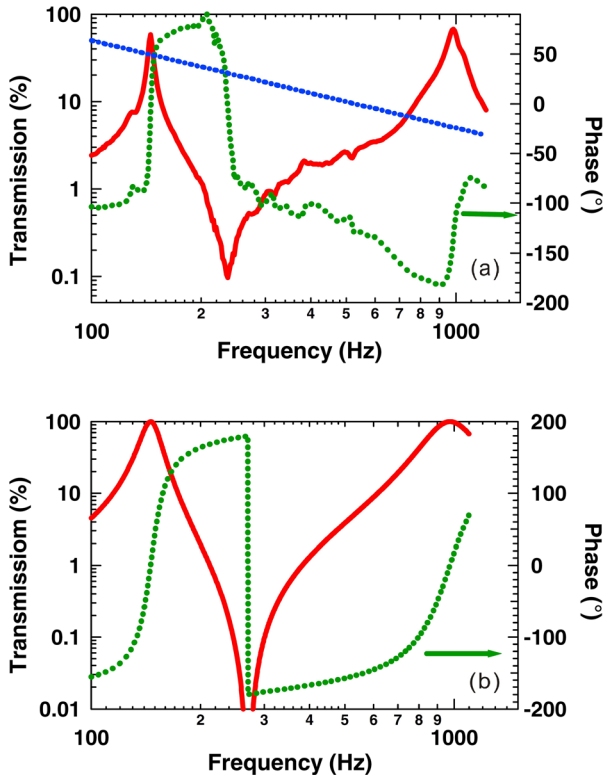


FIG. 4. (Color online) The sound transmission (ratio of the magnitude of the transmitted pressure to the magnitude of the incident pressure in percentage) and the phase of a membrane-type AMM with mass attached are shown. (a) Experimental result. Solid line is the transmission and the dotted line is the phase. The straight dotted line shows the mass law. (b) Numerical result. Solid line is the transmission and the dotted line is the phase. The two resonance frequencies are 146 and 974 Hz where the transmission peaks occur. The anti-resonance frequency is 272 Hz where the transmission dip occurs. Taken from Yang *et al.* (Ref. 39).

rings and distribution of masses were tested both numerically and experimentally. In comparison with the previous studies where the mass weights are placed at the center of the membranes, either the bandwidth of the STL peak was broader or multiple STL peaks could arise. Shortly after, the same group attempted to arrange multiple membrane-type AMMs with masses in a rectangular array to address the scale-up issue of this structures.[47] Multiple arrays were also stacked up to examine the interaction between the layers and improve the STL.[48] In the case of different masses involved, multiple STL peaks occurred correspondingly.

Similar to Ref. 47, Zhang *et al.*[49] also investigated membrane-type AMMs with different or identical attached masses. It was claimed that for membranes carrying different masses, the low-frequency STL can be improved. Zhang *et al.*[50] presented a theoretical model for the membrane-type AMM with a single mass. The inertia force of the mass was treated externally as a concentrated force in the governing equation of the membrane. By applying a normal incident sound wave on the AMM, the STL could be obtained analytically. The effect of varying the position of the mass was also studied and the frequency shift was found to be not significant.

Chen *et al.*[40] developed the theoretical model for circular membrane-type AMMs with multiple, arbitrarily shaped masses. Langfeldt *et al.*[51] also established an analytical model for both circular and rectangular membrane-type AMMs with masses in arbitrary shape. Tian *et al.*[52] introduced a theoretical model for circular membrane-type AMMs with attached rings. Similar to Ref. 11, the inertia force of the ring mass was treated as a concentrated force on the membrane. When the inner radius of the ring increased with a constant weight, the resonance frequencies were found to become higher. The same phenomenon can also be achieved by decreasing the weight of the ring. When multiple rings with different inner radii are present, multiple resonance frequencies can be observed.

Mei *et al.*[53] proposed a different type of membrane-type AMMs (the so-called dark AMMs) which could yield almost 100% acoustic absorption at very low frequencies within a narrow band as demonstrated by their experiments. The proposed AMMs consist of fixed rectangular membranes decorated with semi-circular iron platelets, backed with an aluminum reflector. The underlying mechanism of this dark AMM is that at resonance frequencies, acoustic energy is converted into elastic energy through flapping motion of the platelets and then dissipated efficiently. The resonance frequencies where peak absorption occurs can be tuned by adjusting the weight of the platelet or the separation between two platelets: reducing the lower absorbing frequencies by increasing the weights of platelets; decreasing the higher absorbing frequencies by increasing the separation of platelets.

Chen *et al.*[41] theoretically analyzed the dark AMM under a plane normal incidence by using the modal expansion and point matching methods. The acoustic absorption coefficient can be accurately predicted and microstructure effects were also considered. Ma *et al.*[54] introduced another ultrathin membrane-type AMM (the so-called metasurface) for super-absorption at certain tunable frequencies (Fig. 5). This AMM is comprised of a circular membrane attached with a platelet at the center. The membrane is mounted over a solid surface with sealed gas in between. The reason for the full absorption is that the AMM surface becomes impedance-matched to air at certain frequencies due to hybrid resonances. It was also demonstrated that a high acoustic-electrical energy conversion efficiency of 23% can be achieved using a setup consisting of magnet wires and magnets. Yang *et al.*[55] presented a generalized perspective for understanding the sound absorption and scattering of the membrane-type AMM with masses attached and also experimentally demonstrated perfect sound absorbers based on degenerate decorated membrane resonators.[56]

In contrast to most membrane-type AMMs which only induce negative effective density, Yang *et al.*[57] proposed a membrane-type AMM that could exhibit both negative effective density and negative effective bulk modulus in a relatively broadband frequency range. This device has two membranes (top and bottom) each with a rigid disk attached. The two membranes are connected by a plastic ring and are fixed to a side wall. Two types of resonance modes could be produced by this structure, i.e., the monopolar and dipolar resonances. Under the monopolar resonance, the two disks vibrate out-of-phase and the ring is motionless. Under the dipolar resonance, the two disks vibrate in phase. The ring

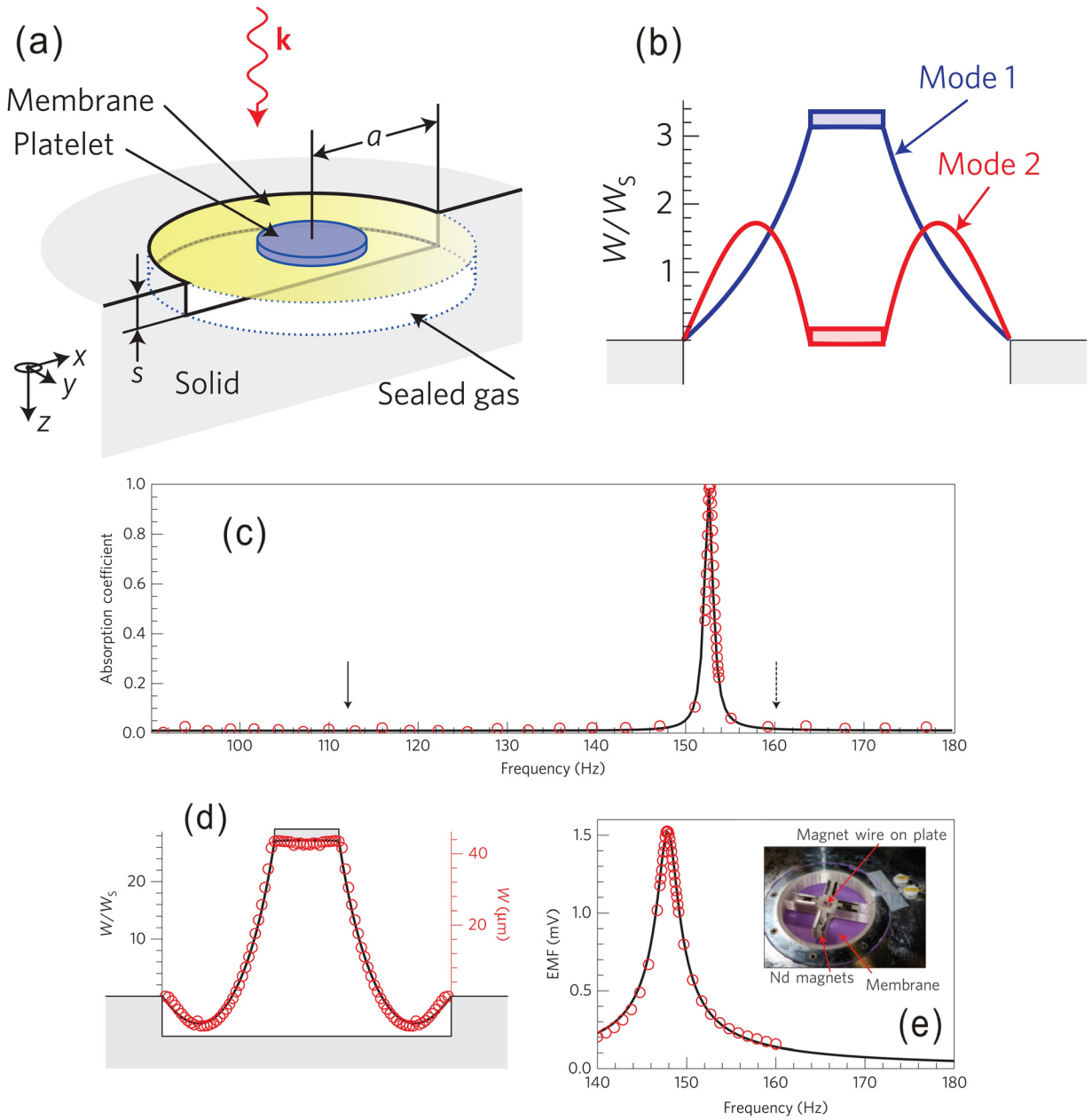


FIG. 5. (Color online) The ultrathin membrane-type AMM (metasurface) for super-absorption. (a) The schematic of the structure. (b) The out-of-plane displacements of the two lowest eigenmodes of the membrane with mass attached. (c) The theoretical (solid line) and experimental (circles) absorption curves. The solid and dashed arrows indicate the first resonance frequency and anti-resonance frequency, respectively. The absorption coefficient is defined by the ratio of the absorbed sound energy to the incident sound energy. (d) The out-of-plane displacements at the absorption peak frequency. (e) The electromotive force generated by the vibration of the AMM. The inset shows the experimental set-up. Taken from Ma *et al.* (Ref. 54).

vibrates either in phase or out-of-phase with respect to the two disks. The monopolar resonance is responsible for the negative effective bulk modulus whereas the dipolar resonance creates the negative effective density. Within the frequency range where monopolar and dipolar resonances overlap, double negativity could be achieved.

Recently, Ma *et al.*[58] fabricated and tested a purely flexible membrane-type AMM. Although the structure looks similar to that in Ref. 39, all materials used are lightweight and flexible, which could be advantageous in practice.

Ma *et al.*[59] designed a membrane-type AMM consisting of four fully clamped membranes with attached disks. A sizable orifice was situated at the center of the material. While this design allows air flow and heat exchange through the orifice, it also yields high STL in a low-frequency narrow bandwidth. It was found that interaction of resonating field of the AMMs with the sound field passing through the orifice is responsible for the large STL.

### B. Plates with masses attached

It has been found that masses attached on plates could also give rise to many intriguing phenomena. Xiao *et al.*[60] theoretically studied the STL through an unbounded thin plate with spring-mass resonators (SMRs) attached using the plane wave expansion method and effective medium method. The

STL of the diffuse sound field was obtained by first solving for the STL at different incident angles. The authors showed that using an extremely thin plate could lead to high STL at low frequencies. Li *et al.*[61] studied multiple layers of thin plate-type AMMs with SMRs attached using the transfer matrix method. Their paper, however, focused more on the effective density of this AMM. Under normal incidence plane wave, they found that the effective density could follow either the Lorentz- or Drude-form model. For oblique angles, the effective density depends on the lateral wave number of the incident wave.

The STL for thick plates with SMRs was obtained theoretically by Oudich *et al.*[62] Unlike the theoretical model in Xiao's paper[60] which only considered flexural waves, a more general case taking other types of elastic waves into account was considered using the plane wave expansion method. Gusev and Wright[63] applied the analytical lumped-element approach to study a double negative meta-plate which exhibited both effective negative density and negative bending modulus for flexural waves. The effective negative density was introduced by normal-force interactions in the resonators vertically attached on the plate. The effective negative bending modulus was achieved by the lateral forces and rotational inertia interactions due to the resonators horizontally attached on the plate.

### C. Membrane- or plate-type AMMs without masses attached

For membrane-type AMMs with mass attached, deep effective negative density in general can only be acquired within a narrow frequency band. In addition, since the negative density is primarily due to resonances, energy loss could become a critical issue. To overcome these limitations, Lee *et al.*[27] proposed low-loss, membrane-type AMMs without mass attached. They placed multiple stretched membranes with a certain separation distance in a waveguide. The edges of the membrane were fixed. The tension on the membrane was calibrated by applying water weight and observing the deformation of the membrane. Negative density was observed below the first resonance frequency of the membrane and the Drude-form effective density was theoretically derived, i.e., Eq. (4). Shortly after, the same group combined this membrane-type AMM with branch openings (side holes) to achieve double negativity,[17] since branch openings can introduce negative bulk modulus.[64,65] A sample was fabricated and tested. The phase velocity was found to be negative under the cutoff frequency of the branch opening $f_{SH}$ and a reversed Doppler effect can be observed.[66] Above the resonance frequency ($f_c$) of the membrane, the AMM is double positive. At a frequency between $f_{SH}$ and $f_c$, the AMM is single negative (only the effective density is negative). Fan *et al.*[67] theoretically and experimentally studied nonlinear wave propagation in this specific type of AMM. The sound pressure amplitude was found to affect the pass and forbidden bands due to the nonlinear effect. This, however, could create opportunities for automatically triggered acoustic isolators and tunable AMMs.

Bongard *et al.*[38] investigated plate-type AMMs without mass attached (Fig. 6). The acoustic impedance of thin plates was first analytically derived. The transmission line approach was then used to estimate the relevant acoustic parameters, including the transmission, phase, and effective medium parameters. Similar to Ref. 16, the effective density was found to be negative below the first resonance frequency of the thin plate. In addition, open channels were adopted to introduce negative bulk modulus. The refractive index can therefore be tuned from negative to zero and to positive. A possible application on directive acoustic sensor (acoustic leaky-wave antenna) was suggested in this paper and was later experimentally validated by Naify *et al.*[68] Meanwhile, Yao *et al.*[29] attempted to use a spring-mass lattice system to explain the negative density below the cutoff frequency. As an example, an elastic 1D waveguide (very thick plate) with clamped boundaries was demonstrated numerically. An array of elastic plates were also fabricated and tested for the sound transmission to show the noise reduction performance in the low frequency region.

Fan *et al.*[69,70] theoretically studied the 1D circular membrane-type AMM with or without branch openings using the fluid impedance theory and Bloch theory to obtain the transmission and dispersion curves. Park *et al.*[26] constructed a 2D membrane-type AMM for amplification of evanescent waves. Such a phenomenon was possible due to the negative effective density resulted from the membrane-type AMM.[71] Potential applications include acoustic superlensing, which was demonstrated recently that showed a resolution at 1/17 of the wavelength thanks to the surface wave stemming from the negative density.[72] Inspired by the electromagnetic wave complementary metamaterials (CMMs), Shen *et al.*[19] designed a quasi-2D acoustic CMM using acoustic coordinate

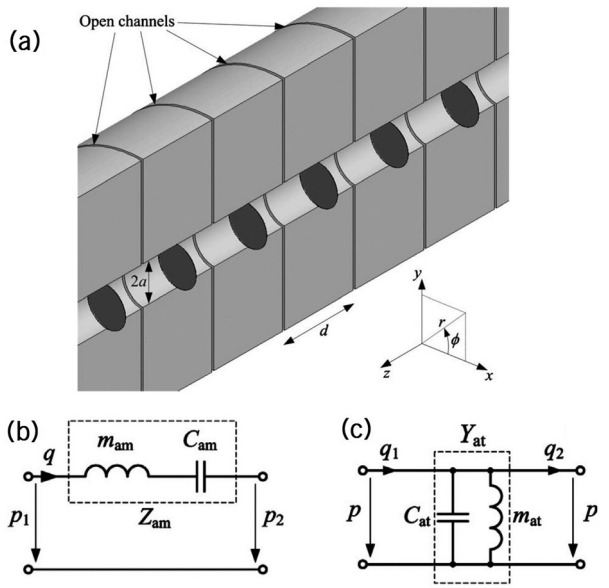


FIG. 6. A plate-type AMM without mass and with radial open channels. (a) The cutaway view of the AMM. (b) The equivalent acoustic circuit for a membrane clamped in the waveguide. The acoustic impedance ($Z_{am}$) of the membrane consists of an acoustic mass ($m_{am}$) and compliance ($C_{am}$) in series. (c) The equivalent acoustic circuit for an open channel. The acoustic admittance $Y_{at}$ consists of an acoustic mass $m_{at}$ and compliance $C_{at}$ in shunt. Taken from Bongard *et al.* (Ref. 38).

transformation (Fig. 7). It was demonstrated that anisotropic, negative density as well as negative bulk modulus required for the acoustic CMMs can be achieved via plate-type AMMs (although the word membrane was used in the paper to describe the thin plate) with branch openings. To create anisotropic effective density, the thin plates facing *x*- and *y*-directions were designed to have different thicknesses. The acoustic CMM was numerically demonstrated to be able to enhance the sound transmission through aberrating layers and reduce the sound field distortion. Such a CMM could allow better sound transmission through the human skull to enable transcranial brain imaging. Most recently, a similar AMM with anisotropic density was proposed to achieve hyperbolic dispersion.[73]

A number of works have been carried out utilizing membrane- or plate-type AMMs for showcasing density near-zero metamaterials (near-zero density typically occurs around the first resonance frequency of the membrane or plate). It was theoretically predicted that[74,75] superlensing can be achieved by using an AMM with anisotropic density: density being near zero in one direction and infinite in another. A superlensing device was designed based on this idea using the plate-type AMM.[75] The authors also pointed out that at the near-zero frequency, all plates in parallel vibrate in phase, giving rise to the uniform phase in the density near-zero AMM. This superlensing effect was recently verified experimentally.[32] The plate material was paper, which has a relatively low energy loss. A resolution of 0.16 wavelengths was demonstrated. Jing *et al.*[31] numerically demonstrated that when a 2D array of plate-type AMMs operate at the density near-zero frequency, only near-normal incident waves can transmit through the AMM, leading to an angular filtering device. This AMM's ability to tailor phase pattern was also shown in the paper. Fleury and Alù[18] also applied the near-zero-density concept to realize extraordinary sound transmission through ultranarrow channels in which membranes were periodically arranged. Numerical simulations were performed. The viscosity effect in the small channel, however, was not considered, which could have a significant adverse impact on the transmission. Park *et al.*[76] constructed walls perforated with sub-wavelength holes and membranes were installed across the holes to introduce zero-mass at certain frequencies. At these frequencies, extraordinary sound transmission can be observed, essentially making a wall "invisible" to sound and could have potential applications in sound filtering and audio microscope. Gu *et al.*[77] designed a 2D network of membrane-type AMMs to demonstrate cloaking, high transmission through sharp corners, and wave splitting at the density-near-zero frequency. Other papers on the topic of membrane- or plate-type AMMs without masses can be found in Refs. 29, 31, and 78–83.

### D. Active AMMs

Active AMM is a concept to give passive AMMs the capability to actively tune the resonance frequency as well as other parameters and was initially introduced and studied by Baz in 2009 (Ref. 84) and 2010.[85] Specifically, the membranes used in the active AMMs were piezoelectric diaphragms and could yield a constant effective density over a wide frequency band. The effective density control was achieved by the active capacitance which resulted from self-sensing feedback, tuning capacitance, and inductance controlled by the applied voltage. Later on, Akl and Baz extended the analysis of tunable effective density from one unit cell to multi-cells.[86] The same authors also created an active AMM with programmable bulk modulus by attaching a piezoelectric diaphragm on the bottom of a resonator cavity (Helmholtz resonator).[87] Their proposed AMMs were experimentally demonstrated,[88,89] which showed that the effective density of the AMM unit cell could be tuned to a value greater than or less than the density of water.

Following the similar working principle in Refs. 88 and 89, Popa *et al.*[90] fabricated two compact unit cells that consisted of a sensing transducer and one or two Lead Zirconate Titanate (PZT) diaphragms. These unit cells were installed in a waveguide to test the performance. In the case of a unit cell with only one PZT diaphragm, the PZT diaphragm was actuated to behave as a dipole source so that the effective mass of the unit cell could be controlled. On the other hand, in the case of a unit cell with two adjacent PZT diaphragms, the two PZT diaphragms were actuated to behave as a monopole source which led to tunable effective bulk modulus. Popa and Cummer[91] also designed, fabricated, and tested highly nonlinear and non-reciprocal active AMMs based on piezoelectric membranes (Fig. 8). The sample consisted of the sensing part, an actuating part, and two subwavelength Helmholtz cavities tuned on different frequencies. A piezoelectric membrane was utilized for sensing and actuating, but essentially behaved as a second harmonic generator (double the incoming wave frequency). The two Helmholtz cavities were responsible for controlling the asymmetrical transmission. An isolation factor of $>10$ dB was observed around 3 kHz. Most recently, the same group built an AMM slab utilizing piezoelectric membranes.[92] They showed that such an AMM can be used as an acoustic lens whose properties are reconfigurable in real time. Imaging at the second harmonics was demonstrated to beat the diffraction limit of the fundamental frequency.

Zhang *et al.*[93] proposed an active plate-type AMM which is composed of a thin plate with shunted piezoelectric patches attached on both sides. STL was calculated by the effective medium method. Compared with the un-shunted case, shunted piezoelectric patches could lead to higher STL. The high STL region can also be broadened by negative capacitance shunting circuits. Other similar papers on active AMMs using piezoelectric elements can be found in Refs. 94–96. Instead of using piezoelectric elements, Chen *et al.*[97] proposed a non-contact method to actively tune the effective density of their membrane-type AMMs. Particles of magnetorheological elastomers were embedded in elastic membranes. Under the external gradient magnetic field, the pre-stress and rigidity of the membrane can be changed so that the resonance frequency can be tuned. Xiao *et al.*[98] proposed a modified membrane-type AMM, which is composed of a metal-coated central platelet on a membrane and a rigid mesh electrode placed above the platelet, to achieve active tuning. With increased direct current voltage applied on the

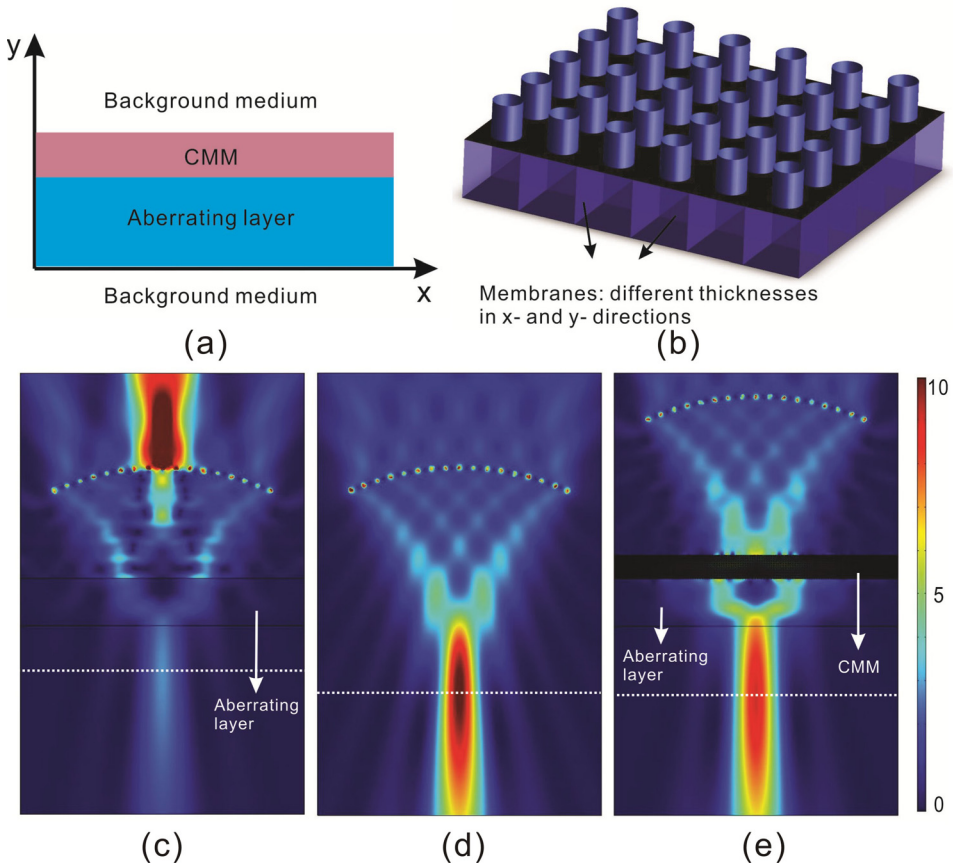


FIG. 7. (Color online) The quasi-2D acoustic CMM. (a) The CMM layer is used to acoustically cancel out the aberrating layer beneath it and to allow better sound transmission. (b) Schematic of the 2D CMM layer. (c) The acoustic intensity field ($W/m^2$) of a focused beam with the aberrating layer only (human skull). (d) The acoustic intensity field ($W/m^2$) of a focused beam in a homogeneous medium (water). (e) The acoustic intensity field ($W/m^2$) of a focused beam with both the CMM layer and the aberrating layer. The sound energy transmitted through aberrating is significantly strengthened thanks to the CMM. Taken from Shen *et al.* (Ref. 19).

mesh electrode and metal-coated platelet, the first eigenfrequency of the membrane and the phase of the transmitted wave can be adjusted. The tunable frequency range was up to 70 Hz. Attaching one passive platelet and one active platelet on a membrane can generate an acoustic switch at the resonance frequency of the active platelet. With phase-matched alternating current voltage applied on the electrodes, the AMM can be an amplifier or a muffler.

Using electroacoustic resonators is another potential method to achieve active AMMs that can potentially inspire

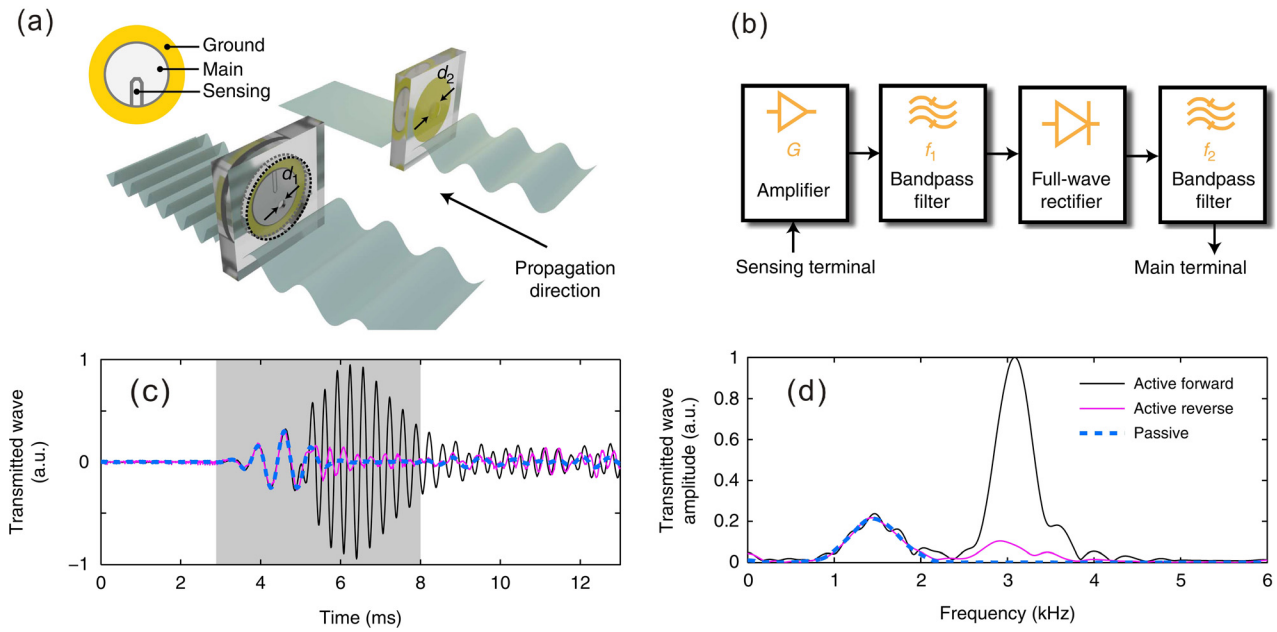


FIG. 8. (Color online) The non-reciprocal active AMM. (a) The unit cell allows acoustic waves to pass in one direction and blocks acoustic waves in the opposite direction. (b) The electronic circuit to drive the membrane using the piezoelectric patch. The transmitted wave vs (c) time and (d) frequency in three cases: cell powered in the forward direction, cell powered in the reverse direction, and unpowered cell. When the cell is powered and the sound is in the forward direction, the transmission is high at the operating frequency, otherwise the transmission is low, leading to the desired non-reciprocity. Taken from Popa *et al.* (Ref. 91).

the development of membrane- or plate-type AMMs. Lissek[99] proposed that an electroacoustic resonator (a loudspeaker) shunted with a series RLC circuit can achieve a feedback-based active impedance control. It has the capability to match acoustic impedance for total absorption or to produce negative acoustic impedance for sound reflection. Fleury *et al.*[100] proposed a parity-time symmetry acoustic sensor by utilizing two loudspeakers. The first loudspeaker connected with a passive electrical circuit absorbs impinging acoustic wave whereas the second loudspeaker connected with an active electrical circuit can produce the time-reversed signal of the first loudspeaker to compensate for the reflected and scattered acoustic field from the first loudspeaker. This acoustic sensor therefore could measure the sound field without affecting it.

## IV. DISCUSSION

Although there has been a substantial development for membrane- and plate-type AMMs, some limitations and challenges should be addressed. The rapid development of these AMMs is largely driven by their potential applications. Out of the many applications proposed by researchers, noise reduction seems to be a particularly promising one. A number of applications, including cloaking,[30] canceling out aberrating layers,[19] super-absorption,[53] and subwavelength imaging,[32] can be challenging to achieve and control in practice due to the requirement of high precision fabrication of the microstructures in order to achieve the accurate effective medium properties of the AMMs. In addition, passive membrane- and plate-type AMMs are liable to strong dispersion, i.e., the effective medium properties are highly frequency dependent. Consequently, most devices targeting these applications operate in a rather narrow frequency band. On the other hand, the noise reduction performance of membrane- and plate-type AMMs do not rely on precise effective medium properties, i.e., as long as the effective density is negative, large STL can be expected. More importantly, due to the lightweight nature of the membrane and thin plate, lightweight noise reduction panels can be designed and constructed to battle low-frequency noise which has been a longstanding issue in both academia and industry. For example, Sui *et al.*[28] experimentally demonstrated that a lightweight thin-plate AMM having a mass per unit area at $1.3\,\mathrm{kg/m^2}$ could yield STL consistently higher than 45 dB below 500 Hz. This type of AMM could be extremely useful in aerospace and automotive industries where weight is considered critical. Previous studies, however, have not validated this type of noise reduction panel on a large scale conforming to standard American Society for Testing and Materials STL testing. The true potential of the AMM based noise reduction panel therefore has yet to be evaluated.

For a majority of membrane-type AMMs, the performance is sensitive to the tension applied to the membrane. Unfortunately, tension is difficult to control and maintain over a long period of time (e.g., tension could change dramatically as time progresses or with a slight variation in temperature or humidity). The requirement of accurate and uniform tension also adds extra complexity to the fabrication process. In this aspect, the plate-type AMMs seem to have an advantage since tension is not required. However, plate-type AMMs could be liable to a greater amount of energy loss, which is undesirable in most applications. This is particularly a problem near the resonance frequency, for example, when the plate-type AMMs are used to achieve near-zero effective density.[31] Consequently, the choice of the plate material is critically important as some materials could be very lossy, such as polymers. In addition, as plate-type AMMs' performance depends on the plate material properties, they could be highly frequency dependent or could vary under temperature change. These facts should be more carefully considered and taken into account by future study on plate-type AMMs.

Three-dimensional (3D) manufacturing of membrane- and plate-type AMMs is also challenging. A number of advanced manufacturing techniques have been utilized for fabricating AMMs, including computer numerical control machining,[101] laser cutting,[12] and 3D printing.[23] However, most membrane- and plate-type AMMs have been fabricated manually, limiting the prototypes to operate at relatively low frequencies. This is partially because the fabrication of membrane- and plate-type AMMs could require multiple different materials simultaneously. This can be potentially circumvented by 3D printing, as some sophisticated 3D printing machines have the capability of printing using multiple different materials. Nevertheless, the precision and resolution of most commercial 3D printers still do not meet the requirement of high frequency AMMs (>100 kHz). Even for kHz range sound, the thickness of membranes or plates could be in the 100 $\mu$m range, challenging the most advanced 3D printers on the market today. More advanced manufacturing technologies therefore need to be developed for high resolution fabrication and mass production of membrane- and plate-type AMMs.


[1]V. G. Veselago, "The electrodynamics of substances with simultaneously negative values of the dielectric constant and the magnetic permeability," Sov. Phys. Usp. **10**(4), 517–526 (1968).
[2]J. B. Pendry, A. J. Holden, D. J. Robbins, and W. J. Stewart, "Magnetism from conductors and enhanced nonlinear phenomena," IEEE Trans. Microwave Theory Tech. **47**(11), 2075–2084 (1999).
[3]J. B. Pendry, "Negative refraction makes a perfect lens," Phys. Rev. Lett. **85**(18), 3966–3969 (2000).
[4]D. Schurig, J. J. Mock, B. J. Justice, S. A. Cummer, J. B. Pendry, A. F. Starr, and D. R. Smith, "Metamaterial electromagnetic cloak at microwave frequencies," Science **314**, 977–980 (2006).
[5]Y. Cui, K. H. Fung, J. Xu, Y. Jin, S. He, and N. X. Fang, "Ultrabroadband light absorption by a sawtooth anisotropic metamaterial slab," Nano Lett. **12**, 1443–1447 (2012).
[6]Z. Liu, X. Zhang, Y. Mao, Y. Y. Zhu, Z. Yang, C. T. Chan, and N. Series, "Locally resonant sonic materials," Science **289**, 1734–1736 (2000).
[7]N. Fang, D. Xi, J. Xu, M. Ambati, W. Srituravanich, C. Sun, and X. Zhang, "Ultrasonic metamaterials with negative modulus," Nat. Mater **5**(6), 452–456 (2006).
[8]G. Ma and P. Sheng, "Acoustic metamaterials: From local resonances to broad horizons," Sci. Adv. **2**(2), e1501595 (2016).
[9]Y. Wu, Y. Lai, and Z.-Q. Zhang, "Elastic metamaterials with simultaneously negative effective shear modulus and mass density," Phys. Rev. Lett. **107**(10), 105506 (2011).
[10]R. Zhu, X. N. Liu, G. K. Hu, C. T. Sun, and G. L. Huang, "Negative refraction of elastic waves at the deep-subwavelength scale in a single-phase metamaterial," Nat. Commun. **5**, 5510 (2014).
[11]R. Zhu, X. N. Liu, G. K. Hu, F. G. Yuan, and G. L. Huang, "Microstructural designs of plate-type elastic metamaterial and their

potential applications: A review," Int. J. Smart Nano Mater. **6**(1), 14–40 (2015).
[12]L. Zigoneanu, B. Popa, and S. A. Cummer, "Three-dimensional broadband omnidirectional acoustic ground cloak," Nat. Mater. **13**, 352–355 (2014).
[13]N. Kaina, F. Lemoult, M. Fink, and G. Lerosey, "Negative refractive index and acoustic superlens from multiple scattering in single negative metamaterials," Nature **525**, 77–81 (2015).
[14]Y. Xie, W. Wang, H. Chen, A. Konneker, B.-I. Popa, and S. A. Cummer, "Wavefront modulation and subwavelength diffractive acoustics with an acoustic metasurface," Nat. Commun. **5**, 5553 (2014).
[15]B. Liang, B. Yuan, and J. Cheng, "Acoustic diode: Rectification of acoustic energy flux in one-dimensional systems," Phys. Rev. Lett. **103**(10), 104301 (2009).
[16]Y. Li, B. Liang, X. Tao, X. Zhu, X. Zou, and J. Cheng, "Acoustic focusing by coiling up space," Appl. Phys. Lett. **101**(23), 233508 (2012).
[17]S. H. Lee, C. M. Park, Y. M. Seo, Z. G. Wang, and C. K. Kim, "Composite acoustic medium with simultaneously negative density and modulus," Phys. Rev. Lett. **104**(5), 054301 (2010).
[18]R. Fleury and A. Alù, "Extraordinary sound transmission through density-near-zero ultranarrow channels," Phys. Rev. Lett. **111**(5), 055501 (2013).
[19]C. Shen, J. Xu, N. X. Fang, and Y. Jing, "Anisotropic complementary acoustic metamaterial for canceling out aberrating layers," Phys. Rev. X **4**(4), 041033 (2014).
[20]P. Sheng, X. X. Zhang, Z. Liu, and C. T. Chan, "Locally resonant sonic materials," Phys. B Condens. Matter **338**(1–4), 201–205 (2003).
[21]B.-I. Popa, L. Zigoneanu, and S. A. Cummer, "Experimental acoustic ground cloak in air," Phys. Rev. Lett. **106**(25), 253901 (2011).
[22]Z. Liang and J. Li, "Extreme acoustic metamaterial by coiling up space," Phys. Rev. Lett. **108**(11), 114301 (2012).
[23]Y. Xie, B. I. Popa, L. Zigoneanu, and S. A. Cummer, "Measurement of a broadband negative index with space-coiling acoustic metamaterials," Phys. Rev. Lett. **110**(17), 175501 (2013).
[24]Z. Liang, T. Feng, S. Lok, F. Liu, K. B. Ng, C. H. Chan, J. Wang, S. Han, S. Lee, and J. Li, "Space-coiling metamaterials with double negativity and conical dispersion," Sci. Rep. **3**, 1614 (2013).
[25]Y. Li, B. Liang, Z. Gu, X. Zou, and J. Cheng, "Reflected wavefront manipulation based on ultrathin planar acoustic metasurfaces," Sci. Rep. **3**, 2546 (2013).
[26]C. M. Park, J. J. Park, S. H. Lee, Y. M. Seo, C. K. Kim, and S. H. Lee, "Amplification of acoustic evanescent waves using metamaterial slabs," Phys. Rev. Lett. **107**(19), 194301 (2011).
[27]S. H. Lee, C. M. Park, Y. M. Seo, Z. G. Wang, and C. K. Kim, "Acoustic metamaterial with negative density," Phys. Lett. A **373**(48), 4464–4469 (2009).
[28]N. Sui, X. Yan, T. Y. Huang, J. Xu, F. G. Yuan, and Y. Jing, "A lightweight yet sound-proof honeycomb acoustic metamaterial," Appl. Phys. Lett. **106**(17), 171905 (2015).
[29]S. Yao, X. Zhou, and G. Hu, "Investigation of the negative-mass behaviors occurring below a cut-off frequency," New J. Phys. **12**, 103025 (2010).
[30]P. Li, X. Chen, X. Zhou, G. Hu, and P. Xiang, "Acoustic cloak constructed with thin-plate metamaterials," Int. J. Smart Nano Mater. **6**(1), 73–83 (2015).
[31]Y. Jing, J. Xu, and N. X. Fang, "Numerical study of a near-zero-index acoustic metamaterial," Phys. Lett. A **376**(45), 2834–2837 (2012).
[32]X. Xu, P. Li, X. Zhou, and G. Hu, "Experimental study on acoustic subwavelength imaging based on zero-mass metamaterials," Europhys. Lett. **109**(2), 28001 (2015).
[33]M. Badreddine Assouar, M. Senesi, M. Oudich, M. Ruzzene, and Z. Hou, "Broadband plate-type acoustic metamaterial for low-frequency sound attenuation," Appl. Phys. Lett. **101**(17), 173505 (2012).
[34]M. Badreddine Assouar and M. Oudich, "Enlargement of a locally resonant sonic band gap by using double-sides stubbed phononic plates," Appl. Phys. Lett. **100**(12), 123506 (2012).
[35]M. Oudich, B. Djafari-Rouhani, Y. Pennec, M. B. Assouar, and B. Bonello, "Negative effective mass density of acoustic metamaterial plate decorated with low frequency resonant pillars," J. Appl. Phys. **116**(18), 184504 (2014).
[36]P. Jiang, X.-P. Wang, T.-N. Chen, and J. Zhu, "Band gap and defect state engineering in a multi-stub phononic crystal plate," J. Appl. Phys. **117**(15), 154301 (2015).
[37]Y. Li, T. Chen, X. Wang, Y. Xi, and Q. Liang, "Enlargement of locally resonant sonic band gap by using composite plate-type acoustic metamaterial," Phys. Lett. A **379**(5), 412–416 (2015).
[38]F. Bongard, H. Lissek, and J. R. Mosig, "Acoustic transmission line metamaterial with negative/zero/positive refractive index," Phys. Rev. B **82**(9), 094306 (2010).
[39]Z. Yang, J. Mei, M. Yang, N. H. Chan, and P. Sheng, "Membrane-type acoustic metamaterial with negative dynamic mass," Phys. Rev. Lett. **101**(20), 204301 (2008).
[40]Y. Chen, G. Huang, X. Zhou, G. Hu, and C. T. Sun, "Analytical coupled vibroacoustic modeling of membrane-type acoustic metamaterials: Membrane model," J. Acoust. Soc. Am. **136**(3), 969–979 (2014).
[41]Y. Chen, G. Huang, X. Zhou, G. Hu, and C. T. Sun, "Analytical coupled vibroacoustic modeling of membrane-type acoustic metamaterials: Plate model," J. Acoust. Soc. Am. **136**(6), 2926–2934 (2014).
[42]G. Ma, "Membrane-type acoustic metamaterials," Ph.D. thesis, The Hong Kong University of Science and Technology, 2012.
[43]S. Yao, X. Zhou, and G. Hu, "Experimental study on negative effective mass in a 1D mass–spring system," New J. Phys. **10**(4), 043020 (2008).
[44]Z. Yang, H. M. Dai, N. H. Chan, G. C. Ma, and P. Sheng, "Acoustic metamaterial panels for sound attenuation in the 50-1000 Hz regime," Appl. Phys. Lett. **96**(4), 041906 (2010).
[45]C. J. Naify, C. M. Chang, G. McKnight, and S. Nutt, "Transmission loss and dynamic response of membrane-type locally resonant acoustic metamaterials," J. Appl. Phys. **108**(11), 114905 (2010).
[46]C. J. Naify, C. M. Chang, G. McKnight, and S. Nutt, "Transmission loss of membrane-type acoustic metamaterials with coaxial ring masses," J. Appl. Phys. **110**(12), 124903 (2011).
[47]C. J. Naify, C. M. Chang, G. McKnight, F. Scheulen, and S. Nutt, "Membrane-type metamaterials: Transmission loss of multi-celled arrays," J. Appl. Phys. **109**(10), 104902 (2011).
[48]C. J. Naify and S. R. Nutt, "Scaling of membrane-type locally resonant acoustic metamaterial arrays," J. Acoust. Soc. Am. **132**, 2784–2792 (2012).
[49]Y. Zhang, J. Wen, H. Zhao, D. Yu, L. Cai, and X. Wen, "Sound insulation property of membrane-type acoustic metamaterials carrying different masses at adjacent cells," J. Appl. Phys. **114**(6), 063515 (2013).
[50]Y. Zhang, J. Wen, Y. Xiao, X. Wen, and J. Wang, "Theoretical investigation of the sound attenuation of membrane-type acoustic metamaterials," Phys. Lett. A **376**(17), 1489–1494 (2012).
[51]F. Langfeldt, W. Gleine, and O. von Estorff, "Analytical model for low-frequency transmission loss calculation of membranes loaded with arbitrarily shaped masses," J. Sound Vib. **349**, 315–329 (2015).
[52]H. Tian, X. Wang, and Y. Zhou, "Theoretical model and analytical approach for a circular membrane–ring structure of locally resonant acoustic metamaterial," Appl. Phys. A **114**(3), 985–990 (2014).
[53]J. Mei, G. Ma, M. Yang, Z. Yang, W. Wen, and P. Sheng, "Dark acoustic metamaterials as super absorbers for low-frequency sound," Nat. Commun. **3**, 756 (2012).
[54]G. Ma, M. Yang, S. Xiao, Z. Yang, and P. Sheng, "Acoustic metasurface with hybrid resonances," Nat. Mater. **13**, 873–878 (2014).
[55]M. Yang, Y. Li, C. Meng, C. Fu, J. Mei, Z. Yang, and P. Sheng, "Sound absorption by subwavelength membrane structures: A geometric perspective," Comptes Rendus Mécanique **343**(12), 635–644 (2015).
[56]M. Yang, C. Meng, C. Fu, Y. Li, Z. Yang, and P. Sheng, "Subwavelength total acoustic absorption with degenerate resonators," Appl. Phys. Lett. **107**(10), 104104 (2015).
[57]M. Yang, G. Ma, Z. Yang, and P. Sheng, "Coupled membranes with doubly negative mass density and bulk modulus," Phys. Rev. Lett. **110**(13), 134301 (2013).
[58]F. Ma, J. H. Wu, M. Huang, W. Zhang, and S. Zhang, "A purely flexible lightweight membrane-type acoustic metamaterial," J. Phys. D. Appl. Phys. **48**(17), 175105 (2015).
[59]G. Ma, M. Yang, Z. Yang, and P. Sheng, "Low-frequency narrow-band acoustic filter with large orifice," Appl. Phys. Lett. **103**(1), 011903 (2013).
[60]Y. Xiao, J. Wen, and X. Wen, "Sound transmission loss of metamaterial-based thin plates with multiple subwavelength arrays of attached resonators," J. Sound Vib. **331**(25), 5408–5423 (2012).
[61]P. Li, S. Yao, X. Zhou, G. Huang, and G. Hu, "Effective medium theory of thin-plate acoustic metamaterials," J. Acoust. Soc. Am. **135**(4), 1844–1852 (2014).
[62]M. Oudich, X. Zhou, and M. Badreddine Assouar, "General analytical approach for sound transmission loss analysis through a thick metamaterial plate," J. Appl. Phys. **116**(19), 193509 (2014).

[63]V. E. Gusev and O. B. Wright, "Double-negative flexural acoustic metamaterial," New J. Phys. **16**(12), 123053 (2014).
[64]C. Shen and Y. Jing, "Side branch-based acoustic metamaterials with a broad-band negative bulk modulus," Appl. Phys. A **117**(4), 1885–1891 (2014).
[65]S. H. Lee, C. M. Park, Y. M. Seo, Z. G. Wang, and C. K. Kim, "Acoustic metamaterial with negative modulus," J. Phys. Condens. Matter **21**(17), 175704 (2009).
[66]S. H. Lee, C. M. Park, Y. M. Seo, and C. K. Kim, "Reversed Doppler effect in double negative metamaterials," Phys. Rev. B **81**(24), 241102 (2010).
[67]L. Fan, Z. Chen, Y. Deng, J. Ding, H. Ge, S. Zhang, Y. Yang, and H. Zhang, "Nonlinear effects in a metamaterial with double negativity," Appl. Phys. Lett. **105**(4), 041904 (2014).
[68]C. J. Naify, C. N. Layman, T. P. Martin, M. Nicholas, D. C. Calvo, and G. J. Orris, "Experimental realization of a variable index transmission line metamaterial as an acoustic leaky-wave antenna," Appl. Phys. Lett. **102**(20), 203508 (2013).
[69]L. Fan, S.-Y. Zhang, and H. Zhang, "Transmission characteristics in tubular acoustic metamaterials studied with fluid impedance theory," Chin.e Phys. Lett. **28**(10), 104301 (2011).
[70]L. Fan, H. Ge, S. Zhang, and H. Zhang, "Research on pass band with negative phase velocity in tubular acoustic metamaterial," J. Appl. Phys. **112**(5), 053523 (2012).
[71]M. Ambati, N. Fang, C. Sun, and X. Zhang, "Surface resonant states and superlensing in acoustic metamaterials," Phys. Rev. B **75**(19), 195447 (2007).
[72]J. J. Park, C. M. Park, K. J. B. Lee, and S. H. Lee, "Acoustic superlens using membrane-based metamaterials," Appl. Phys. Lett. **106**(5), 051901 (2015).
[73]C. Shen, Y. Xie, N. Sui, W. Wang, S. A. Cummer, and Y. Jing, "Broadband acoustic hyperbolic metamaterial," Phys. Rev. Lett. **115**(25), 254301 (2015).
[74]X. Zhou and G. Hu, "Superlensing effect of an anisotropic metamaterial slab with near-zero dynamic mass," Appl. Phys. Lett. **98**(26), 263510 (2011).
[75]A. Liu, X. Zhou, G. Huang, and G. Hu, "Super-resolution imaging by resonant tunneling in anisotropic acoustic metamaterials," J. Acoust. Soc. Am. **132**(4), 2800–2806 (2012).
[76]J. J. Park, K. J. B. Lee, O. B. Wright, M. K. Jung, and S. H. Lee, "Giant acoustic concentration by extraordinary transmission in zero-mass metamaterials," Phys. Rev. Lett. **110**(24), 244302 (2013).
[77]Y. Gu, Y. Cheng, J. Wang, and X. Liu, "Controlling sound transmission with density-near-zero acoustic membrane network," J. Appl. Phys. **118**(2), 024505 (2015).
[78]N. R. Mahesh and P. Nair, "Design and analysis of an acoustic demultiplexer exploiting negative density, negative bulk modulus and extraordinary transmission of membrane-based acoustic metamaterial," Appl. Phys. A **116**(3), 1495–1500 (2014).
[79]N. Cselyuszka, M. Sečujski, and V. Crnojević-Bengin, "Novel negative mass density resonant metamaterial unit cell," Phys. Lett. A **379**(1–2), 33–36 (2015).
[80]S. Varanasi, J. S. Bolton, T. H. Siegmund, and R. J. Cipra, "The low frequency performance of metamaterial barriers based on cellular structures," Appl. Acoust. **74**, 485–495 (2013).
[81]S. Yao, P. Li, X. Zhou, and G. Hu, "Sound reduction by metamaterial-based acoustic enclosure," AIP Adv. **4**(12), 124306 (2014).
[82]Z. Liu, H. Zhang, S. Zhang, and L. Fan, "An acoustic dual filter in the audio frequencies with two local resonant systems," Appl. Phys. Lett. **105**(5), 053501 (2014).
[83]L. Fan, Z. Chen, S. Zhang, J. Ding, X. Li, and H. Zhang, "An acoustic metamaterial composed of multi-layer membrane-coated perforated plates for low-frequency sound insulation," Appl. Phys. Lett. **106**(15), 151908 (2015).
[84]A. Baz, "The structure of an active acoustic metamaterial with tunable effective density," New J. Phys. **11**, 123010 (2009).
[85]A. M. Baz, "An active acoustic metamaterial with tunable effective density," J. Vib. Acoust. **132**(4), 041011 (2010).
[86]W. Akl and A. Baz, "Multicell active acoustic metamaterial with programmable effective densities," J. Dyn. Syst. Meas. Control **134**(6), 061001 (2012).
[87]W. Akl and A. Baz, "Multi-cell active acoustic metamaterial with programmable bulk modulus," J. Intell. Mater. Syst. Struct. **21**(5), 541–556 (2010).
[88]W. Akl and A. Baz, "Experimental characterization of active acoustic metamaterial cell with controllable dynamic density," J. Appl. Phys. **112**(8), 084912 (2012).
[89]W. Akl and A. Baz, "Analysis and experimental demonstration of an active acoustic metamaterial cell," J. Appl. Phys. **111**(4), 044505 (2012).
[90]B. I. Popa, L. Zigoneanu, and S. A. Cummer, "Tunable active acoustic metamaterials," Phys. Rev. B **88**(2), 024303 (2013).
[91]B. I. Popa and S. A. Cummer, "Non-reciprocal and highly nonlinear active acoustic metamaterials," Nat. Commun. **5**, 3398 (2014).
[92]B. I. Popa, D. Shinde, A. Konneker, and S. A. Cummer, "Active acoustic metamaterials reconfigurable in real-time," Phys. Rev. B **91**, 220303 (2015).
[93]H. Zhang, J. Wen, Y. Xiao, G. Wang, and X. Wen, "Sound transmission loss of metamaterial thin plates with periodic subwavelength arrays of shunted piezoelectric patches," J. Sound Vib. **343**, 104–120 (2015).
[94]W. Akl and A. Baz, "Stability analysis of active metamaterial with programmable bulk modulus," Smart Mater. Struct. **20**, 125010 (2011).
[95]W. Akl and A. Baz, "Active acoustic metamaterial with simultaneously programmable density and bulk modulus," J. Vib. Acoust. **135**(3), 031001 (2013).
[96]W. Akl and A. Elsabbagh, "Acoustic metamaterials with circular sector cavities and programmable densities," J. Acoust. Soc. Am. **132**, 2857–2865 (2012).
[97]X. Chen, X. Xu, S. Ai, H. Chen, Y. Pei, and X. Zhou, "Active acoustic metamaterials with tunable effective mass density by gradient magnetic fields," Appl. Phys. Lett. **105**(7), 071913 (2014).
[98]S. Xiao, G. Ma, Y. Li, Z. Yang, and P. Sheng, "Active control of membrane-type acoustic metamaterial by electric field," Appl. Phys. Lett. **106**(9), 091904 (2015).
[99]H. Lissek, "Electroacoustic metamaterials: Achieving negative acoustic properties with shunt loudspeakers," Proc. Mtgs. Acoust. **19**, 030023 (2013).
[100]R. Fleury, D. Sounas, and A. Alù, "An invisible acoustic sensor based on parity-time symmetry," Nat. Commun. **6**, 5905 (2015).
[101]S. Zhang, L. Yin, and N. Fang, "Focusing ultrasound with an acoustic metamaterial network," Phys. Rev. Lett. **102**(19), 194301 (2009).